PNAS RESEARCH ARTICLE | AGRICULTURAL SCIENCES

Chronologically inappropriate morphogenesis (*Chinmo*) is required for maintenance of larval stages of fall armyworm

Xien Chen[a,1,2], Jinmo Koo[a,2,3], Surjeet Kumar Arya[a], and Subba Reddy Palli[a,4]

Affiliations are included on p. 10.

Edited by Lynn Riddiford, University of Washington, Friday Harbor, WA; received June 6, 2024; accepted October 9, 2024

Broad complex (Br-C) and eip93F (E93) transcription factors promote insect metamorphosis from larva to pupa and from pupa to adult, respectively. Recently, chronologically inappropriate morphogenesis (Chinmo) has been proposed as a larval specifier in *Drosophila melanogaster*. However, whether Chinmo is required for larval maintenance in lepidopteran insects, the underlying mechanisms involved in maintaining the larval stage, and its interactions with the JH signaling pathway are not well understood. Here, we used a binary transgenic CRISPR/Cas9 system to knockout *Chinmo* and *Kr-h1* (primary response gene in the JH signaling pathway) in the fall armyworm (FAW). *Kr-h1* knockout induced premature metamorphosis only after L5 (penultimate), whereas *Chinmo* and *Kr-h1* double knockout induced premature metamorphosis in L3. Sequencing and differential gene expression (DEG) analysis of RNA isolated from mutants and single-cell multiome ATAC analysis of *Chinmo*, *Kr-h1*, and *Chinmo* and *Kr-h1* double knockout Sf9 cells revealed that Chinmo participates in chromatin modifications that prevent the promoter accessibility and expression of metamorphosis promoting genes. These results suggest that Chinmo is a larval specifier that plays a major role in preventing metamorphosis in early larval stages by controlling chromatin accessibility near the promoters of genes such as *Br-C* and *E93* required for pupal and adult development.

Chinmo | Krüppel homolog 1 | metamorphosis | chromatin accessibility

Significance

The fall armyworm (FAW) is threatening food security worldwide. CRISPR/Cas9-based genome editing was used to identify genes required for larval development in FAW. Development of *Chinmo* mutant (*Chinmo*-M), *Kr-h1* mutant (*Kr-h1*-M), and double mutant (*Kr-h1/Chinmo*-M) was arrested during L2 to L3, L5 to L6, and L2 to L3 molt, respectively. The expression of metamorphosis genes (*Br-C* and *E93*) increased prematurely in L3, L5, and L2 in the *Chinmo*-M, *Kr-h1*-M, and *Kr-h1/Chinmo*-M, respectively. Chromatin modification genes are differentially regulated in *Chinmo*-M and *Kr-h1/Chinmo*-M but not in *Kr-h1*-M. Single-cell multiome ATAC analysis revealed that Chinmo is involved in chromatin modifications preventing the promoter accessibility of metamorphosis genes. Chinmo is required for early larval development, making it an ideal target for pest management.

Holometabolous insects undergo metamorphosis to change from morphologically and physiologically distinct larvae to pupae and adults. Transitions between these stages are tightly regulated by juvenile hormones (JH), which maintain larval status, and ecdysteroids, which promote metamorphosis (1, 2). The actions of these hormones in controlling developmental transitions include regulating cascades of gene expression and repression events (3). When the JH receptor methoprene-tolerant (*Met*) binds to juvenile hormone, it forms a complex with other cofactors and functions as a transcription enhancer complex. It induces the expression of JH response genes, including the gene encoding the transcription factor Krüppel homolog 1 (*Kr-h1*) (4). JH is present throughout the larval stage to maintain the expression of *Kr-h1* until the last instar. During the larval stage, Kr-h1 suppresses the expression of genes encoding the pupal specifier Broad-Complex (*Br-C*) and the adult specifier eip93F (*E93*) to maintain juvenile status (5, 6). The status quo action of JH and Kr-h1 was revealed by experiments in which precocious metamorphosis was observed in the larval stage when *Met* or *Kr-h1* was knocked down (7–9). However, this precocious metamorphosis occurred only in later instars but not in younger instars. Even in the absence of JH or Met, the larvae or nymphs develop normally until the 2nd instar, and precocious metamorphosis occurs only after the 3rd instar of *Bombyx mori* (10) and *Pyrrhocoris apterus* (11). This led to the hypothesis that a larva must reach a certain instar to gain competence and undergo metamorphosis (11). JH-mediated regulation of metamorphosis occurs only after juveniles have reached competence to undergo metamorphosis (12). These results suggest that JH and Kr-h1 are not the only factors maintaining larval stages (1). Therefore, a knowledge gap exists on how juvenile status is maintained during early larval development when JH and Kr-h1 are dispensable.

Recently, Chinmo (chronologically inappropriate morphogenesis) was proposed as the larval specifier in *Drosophila melanogaster* (13). Chinmo, a BTB-zinc finger protein that functions as a transcription factor, was first identified as a regulator of neuronal temporal identity during postembryonic development of the *D. melanogaster* brain. Neuroepithelium differentiation in late larvae requires transcriptional silencing of *Chinmo* by ecdysone (14). In the absence of Chinmo, early-born neurons adopt the fate of late-born neurons (15). Furthermore, the transition in the expression of *Chinmo* to *Br-C/E93* was essential for proper neuronal and glial cell type specification and maturation in *D. melanogaster* (16).

The authors declare no competing interest.

This article is a PNAS Direct Submission.

[1]Present address: Key Laboratory of Plant Protection Resources and Pest Management of the Ministry of Education, Key Laboratory of Integrated Pest Management on the Loess Plateau of Ministry of Agriculture and Rural Affairs, College of Plant Protection, Northwest A&F University, Yangling 712100, Shaanxi, China.

[2]X.C. and J.K. contributed equally to this work.

[3]Present address: Department of Entomology, University of California, Riverside, CA 92521.

[4]To whom correspondence may be addressed. Email: rpalli@uky.edu.

This article contains supporting information online at https://www.pnas.org/lookup/suppl/doi:10.1073/pnas.2411286121/-/DCSupplemental.

Published November 26, 2024.

This regulatory role of the sequential expression of transcription factors was also demonstrated in other tissues, including imaginal discs, salivary glands, and the epidermis of *D. melanogaster.* Strikingly, when *Chinmo* was knocked down in epidermal cells, puparium cuticle tanning occurred with the precocious expression of *E93* in the first instar larval epidermis. The absence of Chinmo allowed the expression of the pupal specifier *Br-C* and the adult specifier *E93* to promote developmental transition (13). In addition to its regulatory interaction with other temporal specifiers (*Br-C* and *E93*), Chinmo is known as an oncogene (17, 18). Chinmo regulates growth in larval and imaginal tissues in a Br-C-independent and -dependent manner (19). The function of Chinmo as a juvenile specifier also holds true in hemimetabolous insects. When *Chinmo* was knocked down, *Blatella germanica* nymphs underwent premature adult metamorphosis (19). Since JH plays minimal developmental roles in *D. melanogaster* (20), studies in lepidopteran insects where JH plays a critical role in the prevention of metamorphosis could provide information on the function of Chinmo as a larval specifier and its interaction with the JH signaling pathway. In addition, the mechanisms by which Chinmo suppresses pupal and adult specifiers (*Br-C* and *E93*) and regulates gene expression to promote larval growth are still unclear.

In this study, we used a lepidopteran pest, *Spodoptera frugiperda* (fall armyworm, FAW), to investigate the function of Chinmo and its interaction with the JH signaling pathway during development. We developed a binary transgenic CRISPR/Cas9 system in which efficient knockout of the target gene can be achieved by crossing a Cas9-expressing transgenic FAW strain with a sgRNA-expressing transgenic FAW strain (21, 22). Using this system, we knocked out *Chinmo* and *Kr-h1* in FAW. Our results suggest that Chinmo is required to maintain the larval stage and that Kr-h1 functions as a key player to prevent premature metamorphosis. Chinmo suppresses the expression of the *Br-C* and *E93* genes, confirming their regulatory interaction. Single-cell Multiome ATAC + Gene Expression analysis revealed that Chinmo is involved in chromatin modifications to prevent the promoter accessibility and expression of genes that promote metamorphosis.

Results and Discussion

Chinmo Suppresses *Br-C* and *E93* Gene Expression in Sf9 Cells. The major function of Chinmo is its ability to suppress the expression of the pupal specifier *Br-C* and the adult specifier *E93* (13, 19). To determine whether these regulatory interactions also occur in the FAW, we first used ovarian tissue-derived cell line Sf9. *Chinmo* was knocked out or overexpressed in Sf9 cells to determine changes in *Br-C* and *E93* gene expression. The knockout (KO) construct was designed to contain the Cas9 open reading frame (ORF) and a sgRNA sequence targeting the fourth exon of *Chinmo* (Fig. 1*A*). The overexpression (OE) construct comprised the Chinmo ORF (Fig. 1*B*). Similar constructs for *Kr-h1* were also designed and used as a positive control since Kr-h1 is already well characterized for its direct suppressive action on the *Br-C* and *E93* genes by identifying its binding site in the promoters of these genes (5, 6). The *piggyBac*-based plasmid containing the red fluorescent protein marker gene and puromycin antibiotic resistance gene was used as a backbone to design KO and OE constructs (Fig. 1*B*). Each plasmid was transfected with a helper plasmid expressing transposase that induces the insertion of the sequence present in the *piggyBac* plasmid into the host genome (23). Cell lines with stable expression were generated and selected through puromycin treatment. The enrichment of transformed cells was verified by the presence of red fluorescence protein (RFP) (Fig. 1*C*). T7E1 enzyme assays confirmed successful disruption of *Kr-h1* and *Chinmo* in KO cells (*SI Appendix*, Fig. S1*A*). RT–qPCR analysis confirmed overexpression of *Kr-h1* and *Chinmo* in OE cells (*SI Appendix*, Fig. S1*B*). Knockout of Chinmo increased *Br-C* mRNA levels by 4.1-fold and *E93* mRNA levels by 1.8-fold compared to their expression in control cells expressing Cas9 (Fig. 1*D*). However, overexpression of *Chinmo* did not cause a decrease in *Br-C* and *E93* mRNA levels, most likely due to relatively high basal expression levels of *Chinmo* in Sf9 cells (*SI Appendix*, Fig. S1*B*). As expected, the knockout of *Kr-h1* increased *Br-C* mRNA levels by 3.1-fold and *E93* mRNA levels by 2.8-fold compared to their expression in control cells expressing Cas9 (Fig. 1*D*). Overexpression of *Kr-h1* decreased *Br-C* mRNA levels to 0.6-fold and *E93* mRNA levels to 0.3-fold compared to their expression in control cells expressing Cas9. These data demonstrate that Chinmo directly regulates *Br-C* and *E93* genes in FAW. We also measured the expression levels of *Chinmo* in *Kr-h1* KO/OE cells and *Kr-h1* in *Chinmo* KO/OE cells. The results showed that expression levels of *Chinmo* did not change in either *Kr-h1* KO and OE cells. In contrast, expression levels of *Kr-h1* were downregulated (0.5-fold) and upregulated (3.4-fold) in *Chinmo* KO and OE cells, respectively (*SI Appendix*, Fig. S1*C*). These data indicate that there might be a crosstalk between Chinmo and Kr-h1.

Kr-h1 directly binds to the promoters of the *Br-C* and *E93* genes and suppresses their expression (6). To determine whether Chinmo functions in a similar manner in FAW, changes in the activity of *Br-C* and *E93* gene promoters were measured in response to *Chinmo* overexpression in Sf9 cells. The *Br-C* and *E93* gene promoter regions were cloned into the luciferase construct and transfected into Sf9 cells, and their activity was measured using the luciferase assay. Sf9 cells transfected with *Chinmo* OE construct along with *Br-C* promoter-Luc construct showed a decrease in the luciferase activity to 0.5-fold compared to the luciferase activity in control cells transfected with promoter construct alone (Fig. 1*E*). Similarly, Sf9 cells transfected with the *Chinmo OE* construct along with the E93 promoter-Luc construct showed a decrease in the luciferase activity to 0.3-fold compared to the luciferase activity in control cells transfected with the promoter construct alone (Fig. 1*E*). This is similar to the decrease in the luciferase activity detected in Sf9 cells transfected with *Kr-h1* OE construct along with *Br-C* promoter-Luc (0.5-fold) or *E93* promoter-Luc (0.3-fold) constructs (Fig. 1*E*). These results confirm that Chinmo indeed suppresses *Br-C* and *E93* gene expression in FAW, and suggest that similar to Kr-h1, Chinmo may directly repress the promoter activity of these genes. It should be noted that *Chinmo* overexpression did not repress the endogenous expression of *Br-C* and *E93* genes (Fig. 1*D*). The discrepancy between the endogenous gene expression experiment (Fig. 1*D*) and the cloned promoter activity experiment (Fig. 1*E*) might be because *Chinmo* has relatively high basal expression levels in Sf9 cells. Only two-fold upregulation of *Chinmo* gene was detected in *Chinmo* OE cells (*SI Appendix*, Fig. S1*B*), which may have not been enough to affect endogenous *Br-C* and *E93* expression.

Chinmo Is Required for the Larval Development of FAW. We performed in vivo assays to determine whether Chinmo is required to maintain larval stages in FAW. *Chinmo* and *Kr-h1* mRNA levels were determined in staged FAW. *Chinmo* mRNA levels began to increase at 60 h of embryonic development and reached the peak in first instar larvae, and the higher levels were maintained until ecdysis to 3rd instar larval stage. The *Chinmo* mRNA levels increased again to moderate levels in the 3rd instar larvae, and these levels were maintained in the 4th and 5th instar larval stages. The *Chinmo* mRNA levels decreased to a minimum

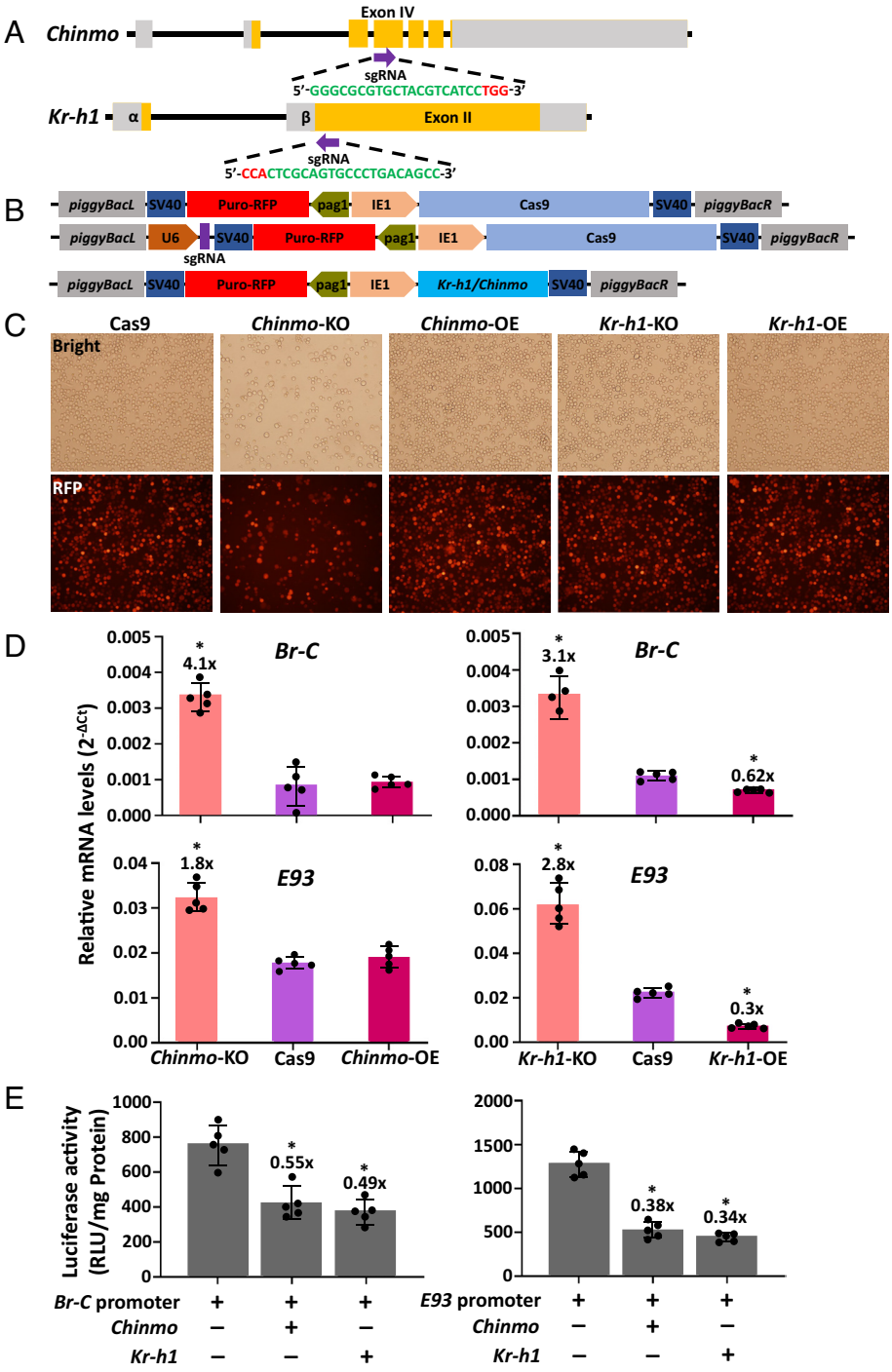

Fig. 1. Knockout (KO) or overexpression (OE) of *Kr-h1* and *Chinmo* in Sf9 cells affects expression of *Br-C* and *E93*. (*A*) Genomic structures of *Kr-h1* and *Chinmo* and sgRNA targeting sites. One sgRNA targeting site located in common Exon II of the α and β isoforms of *Kr-h1* and one sgRNA target site in Exon IV of *Chinmo* were chosen according to the GN19NGG rule. The target and PAM sequences are highlighted in green and red, respectively. (*B*) Schematic representation of the KO and OE constructs of *Kr-h1* and *Chinmo* used for establishing stable Sf9 cells. (*C*) Fluorescence images of stable cells. The transfected Sf9 cells were treated with 100 ng/μL puromycin until all the living cells exhibited RFP signals. (*D*) *Br-C* and *E93* expression in stable Sf9 cells. Total RNA was extracted from Cas9 cells and from KO and OE cells. RT–qPCR was subsequently performed with four biological replicates to evaluate the relative expression levels of *Br-C* and *E93*. Asterisks indicate significant differences between treatment (KO or OE cells) and control (Cas9 cells) based on Student's *t* test. **P* < 0.05. Fold change is indicated on top of the bar. (*E*) Promoter activity assay. The promoter-pG5Luc construct was cotransfected with the *Kr-h1* or *Chinmo* overexpression plasmids into Sf9 cells. The cells were harvested two days posttransfection, after which a luciferase activity assay was conducted. All the data are presented as the means ± SDs (n = 5). Asterisks indicate significant differences between the treatment (Kr-h1 or Chinmo OE) and control (promoter construct only) groups based on Student's *t* test. **P* < 0.05. Fold change is indicated on top of the bar.

in L6, and these lower levels were maintained throughout larval and pupal stages except for a sharp increase during larval–pupal metamorphosis (*SI Appendix*, Fig. S2). The *Kr-h1* mRNA levels also showed a similar expression pattern, except for the additional peak expression during the adult stage. The expression of *Kr-h1* in the late prepupae has been demonstrated to be essential for the formation of the pupa (24). Depletion of this specific *Kr-h1* peak during pupal metamorphosis triggers a direct transformation of the larva into adult form, bypassing the pupal stage (25). The expression of *Chinmo* in the early pupae suggests a function for

this transcription factor in adult development. Further studies are needed to test this hypothesis. Reverse genetic tools, such as RNAi or conditional CRISPR, may be applied to uncover Chinmo's function in adult development in the FAW.

A binary transgenic CRISPR/Cas9 system was established to knockout *Chinmo* and *Kr-h1* genes in FAW. Using the *piggyBac* transposon system (26), transgenic FAWs, including the Cas9 line and sgRNA lines targeting the *Chinmo* and *Kr-h1* genes, were generated (*SI Appendix*, Fig. S3 *A* and *B*). By crossing the Cas9 line and sgRNA line, efficient target gene knockout can be achieved (22). After crossing, we used fluorescent markers to select progeny that expressed both Cas9 (GFP) and the target sgRNA (RFP) (*SI Appendix*, Fig. S3 *B* and *C* and Table S1). The *Chinmo* knockout mutants (*Chinmo*-M) developed normally until L2, and most of these insects died during L3 molt (Fig. 2*A* and Table 1). *Chinmo*-M L3 larvae were stuck inside the old L2 cuticle (Fig. 2*A* and *SI Appendix*, Fig. S4*A*). A small portion of the *Chinmo*-M developed into L4 (Table 1). All the L4 larvae died during molt and could not shed their old cuticle (Fig. 2*A* and Table 1). Even when the old cuticle was removed, the insects did not feed and eventually died. The *D. melanogaster Chinmo* mutant was embryonic lethal. The *Chinmo* mosaic mutant of *D. melanogaster* was able to hatch but died later in the L1 stage. Cuticle tanning was observed on the epidermis of L1, which is a sign of precocious puparium formation (13). These results from *D. melanogaster* indicate that Chinmo is required for larval development and suppression of pupal metamorphosis. From our FAW results, it is difficult to conclude whether Chinmo is required for embryogenesis and larval development before L2. No obvious precocious metamorphosis phenotype was detected in *Chinmo*-M FAW. Since the *Chinmo*-M FAW generated in our study are mosaic mutants, some cells with functional Chinmo may have supported the development of FAW embryo and L1. However, since *Chinmo*-M disrupted larval development in L3, Chinmo is likely required for larval development in FAW.

The *Kr-h1* knockout mutants (*Kr-h1*-M) developed normally until L4 (Table 1). Pupal patches and melanization were observed

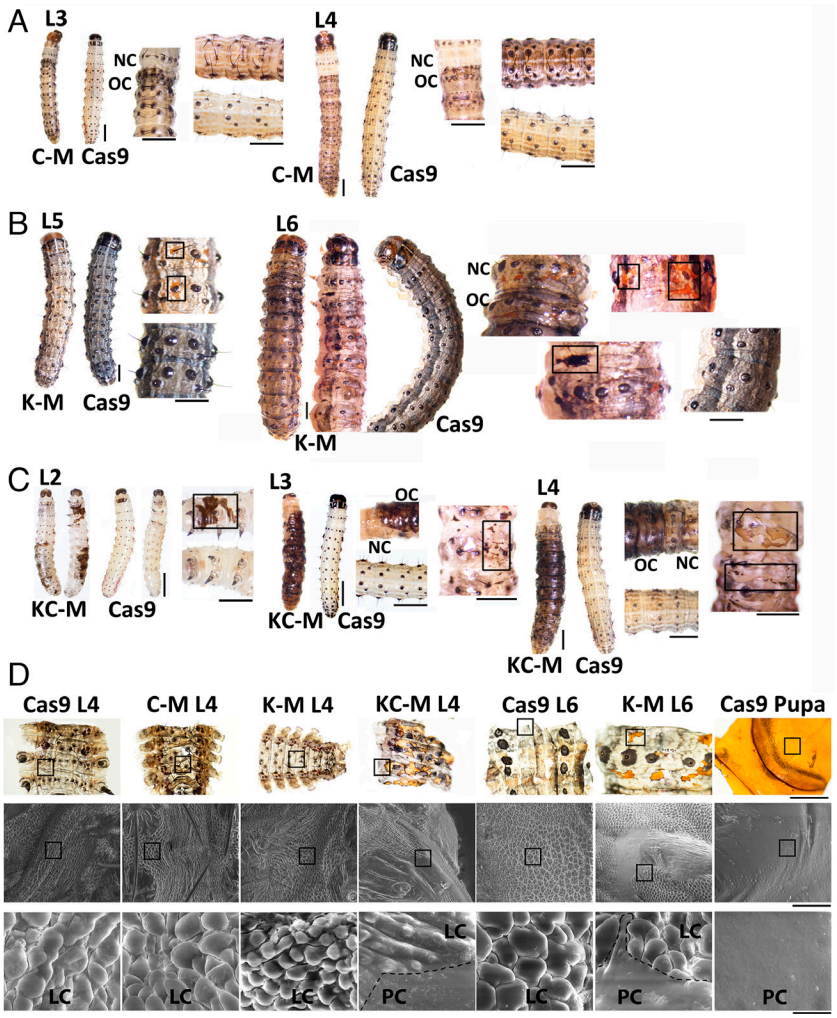

Fig. 2. Phenotypes of *Chinmo*-M (C-M), *Kr-h1*-M (K-M), and *Kr-h1*/*Chinmo*-M (KC-M). (*A*) Representative images of *Chinmo*-M larvae (vertical Scale bar, 1.5 mm; horizontal Scale bar, 0.7 mm). L3 and L4 larvae showing developmental arrest were photographed before and after removing the old cuticles. NC and OC represent new cuticle and old cuticle, respectively. (*B*) Representative images of *Kr-h1*-M animals (vertical Scale bar, 1.5 mm; horizontal Scale bar, 0.7 mm). Most of the *Kr-h1*-M animals completed larval development until L6. Pupal patches were observed in some new L5. Some L6 larvae with clear pupal patches were stuck inside the old L5 cuticle. Pupal patches are marked by rectangles. NC and OC represent new cuticle and old cuticle, respectively. (*C*) Representative images of *Kr-h1*/*Chinmo*-M larvae (vertical Scale bar, 1.5 mm; horizontal Scale bar, 0.7 mm). Several L2 larvae exhibited a severe melanization phenotype (black rectangle). Most L3 were stuck inside the old cuticles. Pupal patches (black rectangle) were detected after removing the old L2 cuticle. All L4 animals were arrested in the old L3 cuticles, and pupal patches were observed under the old L3 cuticles (black rectangle). NC and OC represent new cuticle and old cuticle, respectively. (*D*) SEM analysis of the cuticles from the Cas9 line and mutant line larvae. Cuticles were dissected from L4 of the Cas9 line and three mutant lines, as well as from L6 and pupa of the Cas9 line and from L6 of the *Kr-h1*-M line. Magnified views of the chosen areas are marked by black rectangles. The dotted line represents the boundary between the larval cuticle (LC) and pupal cuticle (PC). (Scale bar, 500 μm, *Top*; 100 μm, *Middle*; 5 μm, *Bottom*)

on the L5 epidermis (Fig. 2*B* and *SI Appendix*, Fig. S4*B*). Most of the larvae died during L6 molt (Fig. 2*B* and Table 1). L6 larvae were stuck inside the old cuticle. When the old cuticle was removed, pupal patches (Fig. 2*B* and *SI Appendix*, Fig. S5) were observed. When those larvae were dissected, pupal fat body and midgut were observed, indicating that they were undergoing precocious metamorphosis (*SI Appendix*, Fig. S6*A*). Few individuals were able to molt successfully and continue to grow during L6 with both pupal patches and melanization spots in the integument (Fig. 2*B*), but they died as deformed prepupae (*SI Appendix*, Fig. S6*B*) or pupae (*SI Appendix*, Fig. S6*C*). Pupal cuticle patches in the larval stage are signs of precocious metamorphosis (10). JH deficiency induces black melanized cuticles in *Manduca sexta* (27). Therefore, the melanization phenotype observed in *Kr-h1*-M indicates that JH signaling has been effectively disrupted. JH disruption caused by *Met* knockout in *Aedes aegypti* also causes precocious metamorphosis accompanied by a melanized cuticle (28). Therefore, our results are consistent with previous findings that disruption of JH signaling induces precocious metamorphosis (9, 28). Our results are also consistent with the previous observations that the metamorphosis suppression function of JH is not required during early larval stages. Disruption of JH signaling induces precocious metamorphosis only in the later larval stages (10, 11).

The *Kr-h1* gene codes for two isoforms (*Kr-h1α* and *Kr-h1β*). We checked whether there was any specificity in the function of these isoforms. These two isoforms exhibited similar developmental expression profiles (*SI Appendix*, Fig. S7*A*). We designed and established a transgenic sgRNA line specific for each isoform (*Kr-h1α*-M and *Kr-h1β*-M) (*SI Appendix*, Fig. S7*B*). By crossing those sgRNA lines with the Cas9 line, we generated *Kr-h1α* (*Kr-h1α*-M) and *Kr-h1β* (*Kr-h1β*-M) mutant strains. Surprisingly, these mutants developed normally (*SI Appendix*, Fig. S7 *C* and *D*). This finding suggested that the presence of either of these isoforms is sufficient for the normal function of the *Kr-h1* gene.

JH signaling is still intact in *Chinmo*-M. We hypothesized that this intact JH signaling pathway may have suppressed precocious metamorphosis phenotype even in the absence of the Chinmo. To test this hypothesis, we established a sgRNA line targeting the Chinmo and *Kr-h1* genes. By crossing this sgRNA line with the Cas9 line, we generated *Chinmo* and *Kr-h1* double knockout mutants (*Kr-h1/Chinmo*-M). Like in *Chinmo*-M, most *Kr-h1/Chinmo*-M died during the L3 molt (Fig. 2*C* and Table 1 and *SI Appendix*, Fig. S4*C*). Some of the late L2 larvae showed melanization of their cuticles (Fig. 2*C*), and as they developed into L3, the melanization became more pronounced (Fig. 2*C* and *SI Appendix*, Fig. S4*D*). The L3 larvae got stuck inside the old cuticle, and when the old cuticle was removed, pupal patches were detected in the cuticles of the L3 larvae (Fig. 2*C*). A small portion of the *Kr-h1/Chinmo*-M developed into L4. All the L4 larvae died during molt and were unable to shed their old cuticle. Severe melanization was observed in this stage. When the old cuticle was removed, we observed clear pupal patches in the cuticles of L4 larvae (Fig. 2*C*).

The phenotypes of *Kr-h1/Chinmo*-M double mutants are similar to the phenotypes observed in the L6 stage of *Kr-h1*-M, except that the same phenotypes could be observed in much earlier stages (L3 and L4) in *Kr-h1/Chinmo*-M double mutant. These findings clearly show that Chinmo is an important factor that suppresses precocious metamorphosis in the earlier stage of FAW. Chinmo is a key player in the maintenance of early larval stages, and the absence of JH action can induce precious metamorphosis only in the absence of Chinmo during later larval stages. However, the fact that this precocious metamorphosis phenotype was observed only after L3 in *Kr-h1/Chinmo*-M double mutants makes it hard to conclude on the function of Chinmo in L1 and L2 stage. Both *Br-C* and *E93* were upregulated in *Kr-h1/Chinmo*-M double mutant larvae of L2 but not L1 (*SI Appendix*, Fig. S13). This lack of effect during earlier stages may be due to the mosaic nature of CRISPR knockouts. It is still possible that unidentified factors, in addition to Chinmo, may be involved in antimetamorphic roles in L1 FAW. Genomic regions containing sgRNA target sites were amplified via PCR. A T7E1 assay with those fragments revealed efficient mutations in all the knockout lines generated in our study (*SI Appendix*, Fig. S8). These fragments were sequenced to confirm the presence of mutations, deletions, and insertions around the sgRNA target sites (*SI Appendix*, Fig. S9).

We used a scanning electron microscope (SEM) to observe the structures of the pupal cuticular patches in the mutants. SEM images revealed clear differences between larval and pupal cuticles. Previous studies in silkworm revealed that larval cuticles have bumps on their surface, whereas pupal cuticles have smooth surfaces (10). Using these structures as key characteristics, we confirmed the presence of pupal patches in *Kr-h1/Chinmo*-M L4 and *Kr-h1*-M L6 (Fig. 2*D*). SEM images also confirmed that the pupal patch-like structure observed in *Kr-h1/Chinmo*-M L3 indeed had a smooth pupal cuticle (*SI Appendix*, Fig. S10). Pupal patches with possible necrosis were also observed in *Kr-h1/Chinmo*-M L3 (*SI Appendix*, Fig. S11). These necrotic-like patches look like broken/lacerated wounds, which is likely the result of strong melanization phenotype.

Molecular Mechanisms of Chinmo and Kr-h1 Interaction. To identify the molecular mechanisms through which Chinmo and Kr-h1 work together to prevent metamorphosis in FAW, we compared the expression of genes involved in JH action in mutants and wild-type. The expression of the JH esterase (JHE) enzyme gene is upregulated in the late last instar larvae; JHE metabolizes JH, which promotes metamorphosis (29–31). *JHE* expression increased during the last instar and reached the maximum levels during pupation (*SI Appendix*, Fig. S12*A*). The expression of both *Br-C* and *E93* increased beginning on the last day of the final instar larval stage and reached the maximum levels during the pupal stage (*SI Appendix*, Fig. S12 *B* and *C*). In *Chinmo*-M, upregulation of *JHE, Br-C*, and *E93* gene expression was detected in 12-h-old L3 (Fig. 3). This could be an indication of precocious metamorphosis, although an obvious phenotype was

Table 1. Phenotypes detected in control (Cas9) and mutant

Genotype	*N*	Larval lethality					Stuck in old cuticle					Pupal patches		
		L2	L3	L4	L5	L6	L2	L3	L4	L5	L6	L2	L3	L4
Cas9	60	0	1	0	0	2	0	0	0	0	0	0	0	0
Kr-h1-M	99	0	2	1	12	84	0	0	0	2	19	0	0	0
Chinmo-M	79	0	58	21			0	55	21			0	0	0
Kr-h1/Chinmo-M	73	2*	54	17			0	54	17			0	42	17

*Two dead larvae showed strong melanization.

not observed in *Chinmo*-M. In *Kr-h1/Chinmo*-M, upregulation of *Br-C* and *E93* gene expression was observed as early as late L2. Moreover, the increase in the expression of these genes in 12-h-old L3 was greater in the *Kr-h1/Chinmo*-M double mutant than in the *Chinmo*-M single mutant (Fig. 3 and *SI Appendix*, Fig. S13). *JHE, Br-C*, and *E93* gene expression did not change in *Kr-h1*-M compared to that in the Cas9 control in the early larval stages (Fig. 3). These results suggest that in the presence of Chinmo, *Kr-h1* knockout alone is unable to induce metamorphosis-related genes in early larval stages. However, in the absence of Chinmo, *Kr-h1* knockout can cause upregulation of metamorphosis-related genes. Prophenoloxidase (PPO) is a key enzyme involved in melanization of cuticle and innate immunity (32, 33). There was no change in *PPO2* gene expression in *Chinmo*-M or *Kr-h1*-M compared to that in the Cas9 control (Fig. 2). However, the *PPO2* gene was upregulated in *Kr-h1/Chinmo*-M as early as in L2 (*SI Appendix*, Fig. S13). These results are consistent with the phenotype data in which melanization was observed only in *Kr-h1/Chinmo*-M. JH acid methyltransferase (JHAMT) is a key enzyme that catalyzes one of the last steps of JH biosynthesis (34, 35). The *JHAMT* gene was upregulated in all the mutants of L3 (Fig. 3). The expression of *JHAMT* may have increased to compensate for the disruption in JH signaling in these mutants. This result is in agreement with previous studies that showed disruption of JH signaling results in an increase in JH biosynthesis (36–38). An increase in *JHAMT* expression is higher in *Kr-h1/Chinmo*-M compared to that in *Chinmo*-M or *Kr-h1*-M, suggesting that compensatory upregulation mechanism in *Chinmo*-M and *Kr-h1*-M are nonredundant. We also found that *Chinmo* expression does not significantly change in *Kr-h1*-M compared to the Cas9 control (*SI Appendix*, Fig. S14*A*). However, the *Kr-h1* gene expression is higher in *Chinmo*-M compared to the Cas9 control (*SI Appendix*, Fig. S14*B*). This provides additional evidence for compensatory increases in JH biosynthesis in larvae deficient in the larval specifier *Chinmo* resulting in upregulation of the primary JH response gene *Kr-h1*. It has been reported that once pupally committed, the tissue initiates pupal differentiation irrespective of the presence of juvenile hormone (39). The phenotypic and molecular characteristics of *Chinmo*-M and *Chinmo/Kr-h1*-M clearly showed that they are attempting to undergo premature metamorphosis, and upregulation of *Kr-h1* may no longer be able to repress this process. In *Kr-h1*-M, upregulation of *Br-C*, *E93*, and *PPO2* was detected in the older larval stage (L4 late to L5) (*SI Appendix*, Fig. S15). These results confirm the phenotypes observed in which precocious metamorphosis was observed in L5 and L6 in *Kr-h1*-M. The *JHAMT* gene was upregulated in most of the stages tested in *Kr-h1*-M (Fig. 3 and *SI Appendix*, Fig. S15), suggesting stage-independent upregulation of *JHAMT* in the absence of Kr-h1.

To test whether JH or 20-hydroxyecdysone (20E) regulates the expression of Chinmo, Sf9 cells were treated with dimethyl sulfoxide (DMSO), Methoprene, 20E, and Methoprene plus 20E, respectively. The expression levels of *Chinmo* were measured in these cells. The results showed that *Chinmo* expression did not change in Methoprene-treated Sf9 cells compared with DMSO-treated Sf9 cells. However, 20E treatment increased its expression by 1.4-fold. When Sf9 cells were treated with both Methoprene and 20E, the expression levels of *Chinmo* increased by 2.6-fold (*SI Appendix*, Fig. S16). These data indicate that two important insect hormones, juvenile hormone, and ecdysone, may cooperatively regulate *Chinmo* expression.

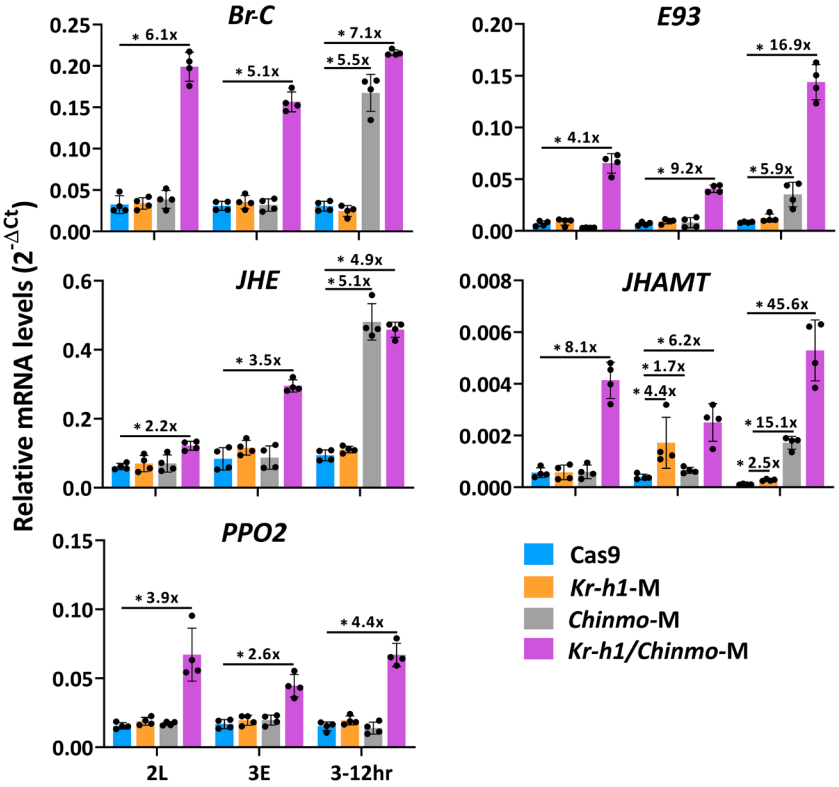

Fig. 3. Comparison of the expression of selected genes in the control and mutant strains. The expression levels of *Br-C, E93, JHE, JHAMT,* and *PPO2* genes were determined in late L2 (2L), early L3 (3E), and 12-h-old L3 (3-12 h) of Cas9 and three mutant lines. The relative mRNA levels normalized against *28S rRNA* are shown. RT–qPCR was conducted using 10-fold diluted cDNAs (1.0 μL) as templates. However, *JHAMT mRNA* was not detectable due to its reduced expression in many samples. Double the volume (2.0 μL) of undiluted cDNA was subsequently used to determine the expression levels of *JHAMT*. The results are presented as the means ± SDs (n = 4). Asterisks indicate significant differences between each mutant and the Cas9 line based on Student's *t* test. The values on the top of the bars represent fold changes. Only the significant changes are shown *$P < 0.05$.

Our RT–qPCR results suggest that Chinmo and JH signaling work together to prevent premature expression of metamorphosis-promoting genes. To further evaluate the global gene expression changes, RNA isolated from Cas9 (control), *Chinmo*-M, *Kr-h1*-M, and *Kr-h1/Chinmo*-M 12-h-old L3 was sequenced, and differential gene expression (DEG) analysis was conducted. There was considerable overlap of DEGs between the *Chinmo*-M and *Kr-h1/Chinmo*-M (*SI Appendix*, Fig. S17). The upregulated DEGs of both the *Chinmo*-M and *Kr-h1/Chinmo*-M were enriched in GO terms related to metamorphosis and development (*SI Appendix*, Table S2). We also compared the transcriptomic data of 12-h-old L3 of *Chinmo*-M, *Kr-h1/Chinmo*-M, and wild-type (WT) pupa (Accession numbers: SRR1196272, SRR11196271, SRR1196269) with 12-h-old L3 Cas9 line (Control). Considerable amount of overlap was detected in the DEGs between those groups. Overlapping upregulated DEGs were enriched in GO terms related to metamorphosis and development (*SI Appendix*, Fig. S18). These data suggest that the genetic program in the mutants resembles the pupal genetic program.

Since both 12-h-old L3 *Kr-h1/Chinmo*-M and 6-h-old-L6 *Kr-h1*-M showed precocious metamorphosis phenotypes, we hypothesized that they would share similar gene expression profiles. Considerable overlap of DEGs was observed not only between 12-h-old L3 *Kr-h1/Chinmo*-M and 6-h-old L6 *Kr-h1*-M but also between 12-h-old L3 *Chinmo*-M (Fig. 4*A*). The expression of genes coding for the larval cuticle proteins was downregulated, and the expression of the genes coding for the pupal cuticle proteins was upregulated in 12-h-old L3 *Kr-h1/Chinmo*-M and 6-h-old L6 *Kr-h1*-M (Group I in Fig. 4*B* and *SI Appendix*, Table S3). Melanization genes (Group II in Fig. 4*B* and *SI Appendix*, Table S3) were upregulated in these mutants. The expression of genes coding for proteins involved in autophagy and apoptosis was upregulated in the mutants. Upregulation of apoptosis genes (31) and autophagy genes (32) during metamorphosis induces programmed cell death in larval tissues. Basic juvenile hormone-suppressible protein-coding genes were upregulated in the mutants (Group III in Fig. 4*B* and *SI Appendix*, Table S3). Juvenile hormone-suppressible protein is a storage protein identified in hemolymph during metamorphosis (40, 41). The expression of these genes in *Chinmo*-M is similar to that in *Kr-h1/Chinmo*-M. However, the degree of upregulation was lower in *Chinmo*-M than in *Kr-h1/Chinmo*-M for some of the genes studied (group III in Fig. 4*B*). These results are consistent with the RT–qPCR data, which showed that *Chinmo* knockout alone is sufficient to upregulate metamorphosis genes. Still, in *Chinmo* and *Kr-h1* double knockout, the degree of upregulation of these genes is higher compared to *Chinmo* knockout. This difference may be one of the reasons why we only observed melanization and a pupal cuticle patch phenotype in *Kr-h1/Chinmo*-M larvae but not in *Chinmo*-M larvae.

Chinmo May Act as a Chromatin Modifier. Our next question was how Chinmo regulates global changes in gene expression. The expression of several regulators that promoted closed chromatin structure was downregulated when *Chinmo* was knocked out (Fig. 4*C* and *SI Appendix*, Table S4). Chromatin assembly factor 1 facilitates the formation of nucleosomes (42). In *D. melanogaster* germline stem cells, chromatin assembly factor 1 prevents the expression of differentiation-associated genes (43). On the other hand, some of the regulators that promote open chromatin structure were upregulated when *Chinmo* was knocked out (Fig. 4*C* and *SI Appendix*, Table S4). The chromatin modification-related protein eaf-1 is a component of the NuA4 histone acetyltransferase complex, which is involved in the transcriptional activation of target genes (44). Indeed, according to the RNAseq data, *Chinmo*-M had more upregulated DEGs than downregulated DEGs (Fig. 4*A*). These results suggest that Chinmo may suppress metamorphosis-promoting genes by regulating chromatin accessibility. To test this hypothesis, we performed multiomics (single-cell multiome ATAC + gene expression) analysis in Sf9 cell line developed from FAW ovary. *Chinmo*, *Kr-h1,* and both *Chinmo and Kr-h1* were knocked out in these cells (*Chinmo*-KO, *Kr-h1*-KO, and *Kr-h1/Chinmo*-KO) (Fig. 1). The knockout cells were used in single cell multiome analysis. In each treatment, the cells were clustered based on the expression of the Cas9 gene (*SI Appendix*, Fig. S19). Cells that did not express Cas9 were removed, and the cells expressing Cas9 were selected for further analysis. This approach ensured that only knockout cells were included in the analysis. We first estimated nucleosome signals. TSS (transcription start site) enrichment was calculated using selected TSS positions (*SI Appendix*, Fig. S20). Peaks were called and annotated for the chosen TSS positions. Global differential accessibility analysis revealed that there were more reads mapped to peaks in the *Chinmo*-KO and *Kr-h1/Chinmo*-KO cells (*SI Appendix*, Fig. S21), suggesting that Chinmo promotes closed chromatin configuration. We next examined the chromatin accessibility of specific genes. More reads were mapped to the peaks identified in the promoter regions of the *Br-C* and *E93* genes in the *Chinmo*-KO cells than in the *Kr-h1*-KO cells (Fig. 5 *A* and *B*), indicating that Chinmo suppresses the chromatin accessibility of the promoters of *Br-C* and *E93* genes. We conducted a comprehensive motif analysis of the promoter regions to gain insight into potential regulatory elements. This analysis revealed significant motif occurrences in these regions (*SI Appendix*, Fig. S22). We also found several genes that were upregulated in the absence of Chinmo in both larvae and Sf9 cells. Among these genes, more reads were mapped to peaks identified in the promoter region in the *Chinmo*-KO and *Kr-h1/Chinmo*-KO cells than in the *Kr-h1*-KO cells (*SI Appendix*, Table S5). Taken together, our multiomics analysis suggests that Chinmo participates in the regulation of chromatin remodeling of metamorphosis-promoting genes, such as *Br-C* and *E93*.

The phenotype and gene expression data obtained in our studies suggest that Chinmo is a major player in maintaining the larval stage and preventing metamorphosis. The presence of Chinmo during early larval stages was sufficient to prevent precocious metamorphosis even when the JH signaling pathway was disrupted (*Kr-h1*-M). Knockout of a key gene involved in JH signaling induced precocious metamorphosis only after *Chinmo* gene expression decreased in late L5 (Fig. S2). The *Chinmo* knockout was sufficient to induce the expression of metamorphosis genes but not for inducing metamorphosis phenotypes. *Chinmo* and *Kr-h1* double knockout induced expression of metamorphosis genes and severe precocious metamorphosis phenotypes. These results suggest that Chinmo is the major player in maintaining the early larval stages. In later larval stages, when *Chinmo* gene expression decreases, JH signaling becomes the major player that prevents metamorphosis. JH analog treatment in lepidopteran insects prevents metamorphosis and induces extra larval molt (45, 46). However, the interaction between Chinmo and JH signaling may be more complex than previously thought. A recent study in *Tribolium castaneum* showed that JH maintains *Chinmo* expression (47). The developmental expression of *Chinmo* is similar but not identical to that of *Kr-h1* in FAW (*SI Appendix*, Fig. S2). These results suggest that in FAW *Chinmo* gene expression may be under the control of JH and other unknown factors. We also observed compensatory upregulation of the JH biosynthesis enzyme *JHAMT* in the absence of both Chinmo and Kr-h1 (Fig. 3 and *SI Appendix*, Fig. S13), suggesting a close interaction between Chinmo and JH signaling.

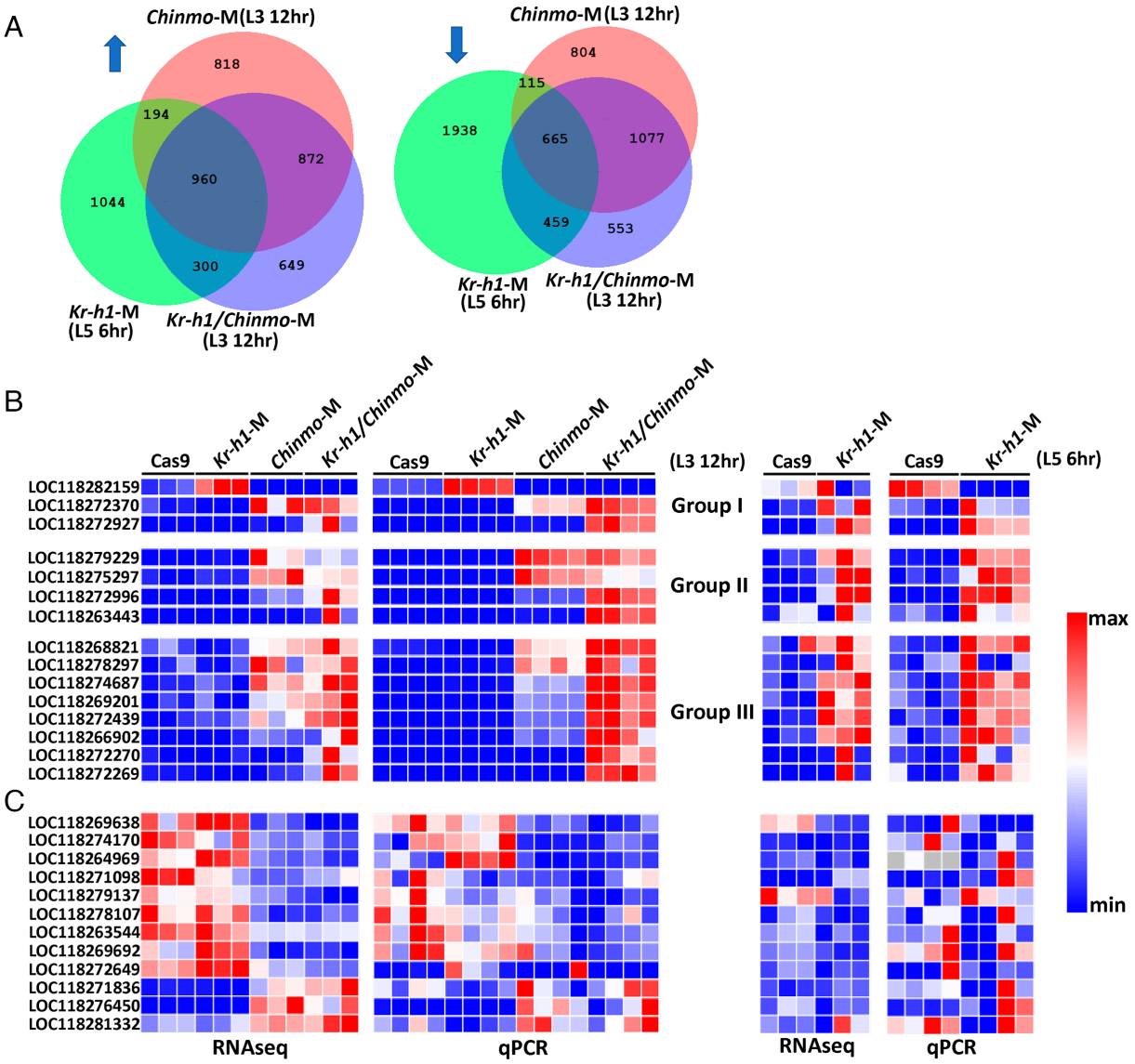

Fig. 4. Comparison of gene expression in mutants by RNAseq and RT–qPCR. (*A*) Venn diagram of common upregulated (*Left*) and downregulated (*Right*) genes in the *Chinmo*-M 12-h-old L3 (L3 12 h), *Kr-h1/Chinmo*-M 12-h-old L3 (L3 12 h), and *Kr-h1*-M 6-h-old L6 (L5 6 h) lines compared with the control Cas9 line in the respective stages. The numbers in the overlapping regions indicate DEGs common to mutants. (*B*) RT–qPCR validation of the expression of selected genes from common DEGs. Heatmap of RNAseq TPM values and RT–qPCR quantification in 12-h-old L3 Cas9 and mutant lines (*Left*) and L5 6 h Cas9 and mutant larvae (*Right*). A description of the selected genes is available in *SI Appendix*, Table S3. (*C*) Differences in the expression of chromatin remodeling genes selected from among the DEGs of 12-h-old L3 Cas9 and mutant lines (*Left*) and L5 6 h Cas9 and mutant larvae (*Right*). A description of the selected genes is available in *SI Appendix*, Table S4.

Chinmo knockout is lethal in L3 (Fig. 2*A* and Table 1), suggesting that Chinmo is required for larval development. Chinmo is a pro-oncogene (17) and is required for regenerative activity in the imaginal discs of *D. melanogaster*. Once the critical weight is reached, ecdysone signaling silences *Chinmo* and activates *Br-C* to switch wing epithelial progenitors from a default self-renewing state to a differentiation state (18). These reports suggest that larval growth may depend on the proliferative function of Chinmo. In *D. melanogaster*, depletion of both Br-C and Chinmo rescued the abnormalities caused by depletion of Chinmo in the wing discs but not in the salivary glands (19). This suggests that the inhibition of larval tissue growth in Chinmo-depleted larvae is not caused by the ectopic upregulation of differentiation-promoting genes such as *Br-C* but rather by the depletion of Chinmo itself. Our results are consistent with these previous observations, suggesting the requirement of Chinmo for larval tissue growth. The downregulated DEGs in the *Chinmo* knockout larvae were enriched for ribosome function and translation (*SI Appendix*, Table S2), further supporting the function of Chinmo in cell proliferation. Some Chinmo knockout L3 could molt to L4, however, they stopped feeding and died (Table 1), indicating that Chinmo also functions in physiological processes other than cell proliferation.

We investigated the mechanism through which Chinmo regulates target gene expression using Sf9 cells. We first showed that Chinmo suppresses the activity of the *Br-C* and *E93* promoters, which were cloned and inserted into reporter constructs (Fig. 1), suggesting that Chinmo may directly suppress these genes. Multiomics analysis showed that Chinmo regulates chromatin accessibility of metamorphosis genes such as *Br-C* and *E93* (Fig. 5). Chinmo may affect the chromatin status near the promoters of metamorphosis-promoting genes such as *Br-C* and *E93*, making them inaccessible to transcription factors, the transcriptional machinery, and other DNA-binding proteins, resulting in a reduction in their expression. Kr-h1 directly suppresses the activity of the *Br-C* and *E93* promoters (6, 48). This is known as a major mechanism in which JH signaling prevents premature

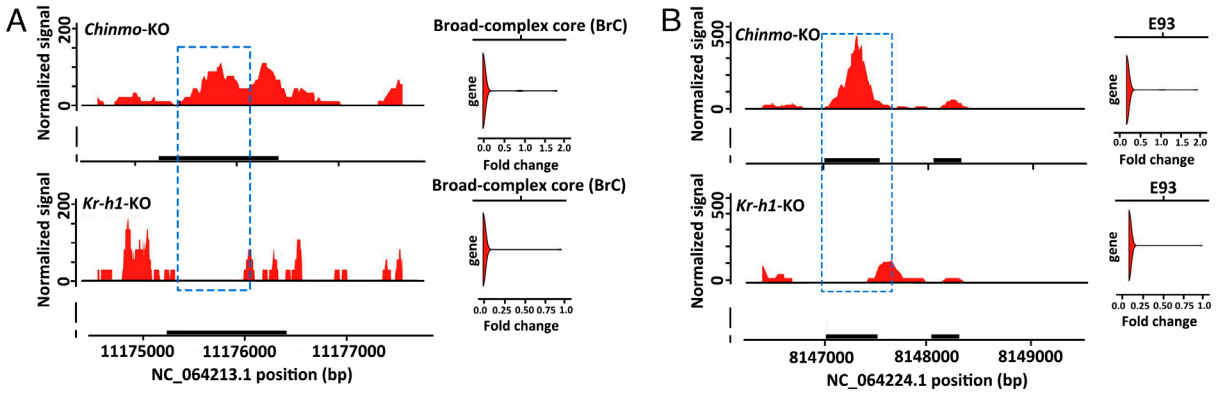

Fig. 5. Multiome analysis of *Chinmo*-KO, and *Kr-h1*-KO Sf9 cells showed differences in the accessibility of *Br-C* (*A*) and *E93* (*B*) promoters. Piles of reads are mapped to the promoter region of the *Br-C* and *E93* genes. The Y-axis represents the normalized signal, while the X-axis represents the chromosomal positions. The graphs on the right show the gene expression levels.

metamorphosis. However, this regulatory mechanism may not be required in the early larval stages when the *Chinmo* expression levels are high, when the *Br-C* and *E93* promoters are inaccessible. In the late larval stages, when the *Chinmo* levels are low, JH signaling and direct suppression by Kr-h1 may be required to prevent metamorphosis. The pupal specifier Br-C and the adult specifier E93 are also known to exert their effects by altering the chromatin landscape near promoters of genes known to be involved in metamorphosis (49). E93 specifies temporal identity by directly regulating the accessibility of temporal-specific transcriptional enhancers (50, 51). Further studies on how Chinmo regulates chromatin accessibility will provide insights into the intricate regulatory mechanisms governing gene expression and chromosomal accessibility during insect development and metamorphosis.

Materials and Methods

Insects and Cell Lines. The FAW strain was purchased from Benzon Research, Inc. (Pennsylvania), and was raised in our laboratory for more than four years. The larvae were fed an artificial diet purchased from Southland Products, Inc. (Arkansas), and the adults were fed a 10% sucrose solution. The larvae and adults were reared at 27 ± 1 °C, 50 ± 10% humidity, 23 ± 1 °C, and 70 ± 10% humidity, respectively. Sf9 cells were cultured in Sf-900 II medium (Thermo Fisher) and maintained at 27 °C.

Plasmids. The plasmids used for establishing stable Sf9 cell lines were constructed based on pBac: hr5ie1-EGFP-SV40: ie1-Cas9-SV40 (gifted from Dr. Anjiang Tan and Dr. Yongping Huang, Shanghai Institute of Plant Physiology and Ecology, China). The luciferase ORF in the pag1-pG5luc vector (52) was replaced with a PuroRFP cassette (synthesized by Integrated DNA Technologies) to produce the pag1-PuroRFP construct. The pag1-PuroRFP-SV40 cassette was subsequently amplified from this vector to replace the hr5ie1-EGFP-SV40 cassette in the pBac: hr5ie1-EGFP-SV40: ie1-Cas9-SV40 plasmid, which yielded the pBac: pag1-PuroRFP-SV40: ie1-Cas9-SV40 (PuroRFP/Cas9) construct. The U6-sgRNA cassette was generated as described previously (26) and inserted into the PuroRFP/Cas9 construct to produce the knockout plasmid pBac: pag1-PuroRFP-SV40: ie1-Cas9-SV40: U6-sgRNA. To create the overexpression plasmids, the ORF of *Chinmo* and the common coding sequence of two *Kr-h1* isoforms were amplified and subsequently used to replace the Cas9 ORF in the pBac: pag1-PuroRFP-SV40: ie1-Cas9-SV40 construct. The ORF of hyperactive *piggyBac* transposase replaced the luciferase ORF in the pag1-pG5luc vector to produce a helper plasmid facilitating transgenesis in Sf9 cells. A transgenic Cas9 line with GFP expression was recently established in our laboratory (22). To produce transgenic sgRNA lines with RFP expression, the ORF of tdTomato was amplified from the ptdTomato Vector (TaKaRa). EGFP in the pBac: hr5ie1-EGFP-SV40 plasmid (21) was replaced with tdTomato to produce the pBac: hr5ie1-tdTomato-SV40 plasmid. The U6-sgRNA cassettes were amplified using PCR as described previously (26) and subsequently inserted into the pBac: hr5ie1-tdTomato-SV40 plasmid to generate the pBac: hr5ie1-tdTomato-SV40: U6-sgRNA plasmid. The fragment was inserted into the plasmid by homologous recombination using Gibson Assembly Master Mix (NEB). All plasmid DNAs were purified using the plasmid midi kit (Qiagen) and stored at −20 °C. The primers used to make the constructs are listed in *SI Appendix*, Table S6.

RNA Isolation, cDNA Synthesis, and RT–qPCR. Wild-type FAW at different developmental stages was collected for gene expression analysis. Knockout FAW lines and Cas9 lines at chosen developmental stages were collected to evaluate changes in gene expression. All the samples were kept at −80 °C until use. Total RNA was extracted from FAW and Sf9 cells with TRI reagent (Molecular Research Center, Inc.) and converted to cDNA using Moloney murine leukemia virus (M-MLV) reverse transcriptase (Invitrogen). RT–qPCR was carried out in a 10-μL total reaction mixture containing 5 μL of 2× SYBR mix (Bio-Rad), 0.4 μL of each primer, 1.0 μL of 10-fold diluted cDNA, and 3.4 μL of double-distilled water. The reaction conditions were as follows: 95 °C for 2 min; 40 cycles of 95 °C for 10 seconds and 60 °C for 1 min. The 28S rRNA and GADPH genes were used as reference genes. Three biological replicates were used for each sample for analyzing the developmental gene expression profile, and the procedure was repeated twice. Four biological replicates were used for each sample for gene expression change analysis between mutants. Primer3 (https://primer3.ut.ee/) was used to design the RT–qPCR primers shown in *SI Appendix*, Table S6.

Cell Transfection and Establishment of Stable Sf9 Cell Lines. Sf9 cells were seeded in 6-well culture plates at a density of 5×10^6 cells per well. The knockout and overexpression plasmids (1.0 μg) and the helper plasmid (0.5 μg) were mixed with 1.5 μL of TransIT-PRO Transfection Reagent (Mirus Bio) and added to each well. Two days posttransfection, the medium was replaced with 2 ml of fresh medium containing 100 ng/μl puromycin (InvivoGen). The puromycin-resistant cells were selected by four rounds of exposure to fresh medium containing 100 ng/μL puromycin every three days. The stable cell lines were maintained in medium supplemented with 20 ng/μL puromycin. The candidate *Br-C* and *E93* promoters were amplified, cloned, and inserted into pG5Luc to drive luciferase expression for promoter activity assays. Sf9 cells were seeded in a 96-well plate at a density of 2×10^5 cells per well. Then, 0.1 μL of TransIT-PRO Transfection Reagent, 100 ng of the promoter-pG5Luc construct and the *Kr-h1* or *Chinmo* overexpression plasmid were added to each well. The cells were harvested at two days post transfection. A luciferase activity assay was conducted as described previously (53) to determine the activity of the *Br-C* and *E93* promoters.

Development of Transgenic FAW Lines and Target Gene Knockout Lines. Germline transformation of FAW was carried out as described previously (21). The fresh embryos (less than 4 h after oviposition) were injected with a mixture of hyperactive transposase mRNA (400 ng/μL) and each *piggyBac* construct (300 ng/μL). The hatched larvae (G0) were reared under normal conditions. The neonates (G1) from crossing G0 female adults with male adults were screened under a stereomicroscope with the fluorescence adapters SFA-RB and SFA-GR (NIGHTSEA) to select transgenic Cas9 animals with GFP signals and transgenic sgRNA animals with RFP

signals, respectively. The positive G1 adults were then crossed with wild-type adults, and the progeny were screened to identify positive G2 animals. To generate target gene knockout animals, G2 Cas9-expressing adults were crossed with G2 sgRNA-expressing adults to produce G3 neonates, and larvae expressing both GFP and RFP signals were used for further analysis. The Cas9 line and sgRNA lines were maintained as heterozygous or homozygous. The transgenic animals were crossed with wild-type animals once every five generations to avoid reduced fecundity.

Phenotyping and Genotyping. The phenotypes of the mutants were observed under a stereomicroscope (Nikon SMZ745T), and electron microscopy was conducted as previously described (28). For genotype analysis, the fragments flanking the sgRNA target sites were amplified using the genomic DNA of the mutant animals as templates. Then, the purified PCR products were subjected to T7E1 as described previously in the field (27) or cloned and inserted into the pMD19-T vector (TaKaRa) and sequenced at Functional Biosciences (Madison, WI).

RNA Sequencing. Total RNA from 12-h-old L3 Cas9, *Kr-h1*-M, *Chinmo*-M, and *Kr-h1/Chinmo*-M FAW and from 6-h-old L5 Cas9 and *Kr-h1*-M FAW were isolated and sequenced (RNAseq) at Beijing Genomics Institute (Beijing, China). The libraries were prepared and sequenced using the BGISEQ-500 NGS platform. Sequenced raw reads were analyzed on a CLC Genomic Workbench (version 9.5.9; Qiagen Bioinformatics, Valencia, CA) employing standard preoptimized settings and parameters as described previously (54). After adaptor removal, the raw reads were mapped to the FAW genome (ZJU_Sfru_1.1 from NCBI). The TPM (transcripts per million) was calculated to determine the expression of genes. DEG analysis was performed with a cutoff value of FDR < 0.05 to identify genes that are differentially expressed in the mutants. The TPM value for the gene of interest was visualized by generating a heatmap using Morpheus (https://software.broadinstitute.org/morpheus/). Gene ontology (GO) analysis was performed in ShinyGO 0.77 (http://bioinformatics.sdstate.edu/go/). FAW genes were blast searched in *D. melanogaster* database and *D. melanogaster* orthologs were used as input for the GO enrichment analysis. All raw reads from the RNAseq analysis were deposited in the NCBI Sequence Read Archive (SRA) under the Bioproject Accession number, PRJNA1168504 (55).

Single-Nucleus Isolation. Treated Sf9 cells were collected by centrifugation for 5 min (at 500 RCF at 4 °C), washed twice with suspension solution (0.05% BSA in 1X PBS), and filtered using a 40 μm cell strainer. The cell concentration was determined using a hemocytometer. Nuclei were isolated following the manufacturer's instructions (10X Genomics, protocol CGOOO338). Before using them for library construction, isolated nuclei were washed with wash buffer and nuclei buffer, and their integrity was checked under a microscope.

Sequencing and Genome Alignment. Sequencing was performed at the University of Kentucky Core Facility, where cDNA libraries were prepared at the imaging center using Chromium Single-cell Multiome ATAC + Gene Expression Reagent Kits and sequenced on Illumina NovaSeq instruments. Demultiplexing, genome alignment, and feature-barcode matrix generation were performed using the 10X Genomics Cell Ranger-arc software pipeline (56). All raw reads from the multiomics analysis were deposited in the NCBI Sequence Read Archive (SRA) under the Bioproject Accession number, PRJNA1168511(57).

Single-Cell Data Analysis. The single-cell multiomics data were analyzed using the open-source Seurat and Signac packages implemented in the R computing environment (58). Comprehensive in-house multiomics analysis pipeline using the Seurat package and related tools were used. The pipeline includes data acquisition, preprocessing, package loading, RNA count extraction, essential annotation incorporation from the GTF (General Transfer Format) file, quality control, nucleosome signal extraction, curation of high-quality cells, extraction of transcription start site (TSS) positions, TSS enrichment score computation, peak calling using MACS2 (59), quantification of counts within each peak, annotation of peaks with their nearest genes, and extraction of gene-related information. A custom GTF file containing reference markers was created by manually adding the gene information of Cas9 (LOCCas9), puromycin (LOCpuro), and red fluorescent protein (LOCRED) expression sequences using guided instructions from the 10X Genomics Cell Ranger-arc in both the genome fasta and the GTF files. Normalization and dimensional reduction techniques such as TF–IDF (Term Frequency–Inverse Document Frequency), SVD (Singular value decomposition), and UMAP (uniform manifold approximation and projection) were applied to reduce noise and emphasize meaningful features for exploratory data analysis. Clustering results were visualized, and coverage plots for promoter regions of genes of interest (LOC118273024; *Chinmo*), (LOC118269059; *Br-C*), and (LOC118270242; *E93*) were generated to represent the distribution of sequencing reads across genomic regions, providing insights into gene accessibility and expression patterns.

Motif Analysis using the MEME Suite. To harness motif information, we leveraged computational databases containing motif sequences. We utilized the comprehensive JASPAR database (60), which encompasses motifs from multiple species and is easily accessible through application programming interfaces (APIs) or Bioconductor packages (61, 62). In our analysis, we employed the Multiple EM for Motif Elicitation (MEME) suite, which includes the Tomtom tool for searching for individual motifs (63). With these tools, the position and frequency of motifs within each identified peak region were determined. This motif analysis is a crucial step in deciphering potential regulatory elements and understanding the intricate mechanisms governing chromosomal accessibility under our experimental conditions.

Data, Materials, and Software Availability. RNA seq data have been deposited in NCBI (PRJNA1168504 and PRJNA1168511 released after publication) (55, 57).

ACKNOWLEDGMENTS. We thank Jeff Howell from the University of Kentucky for helping with FAW rearing. The Agriculture and Food Research Initiative Competitive Grant No. 2019-67013-29351 and the National Institute of Food and Agriculture, US Department of Agriculture (2353057000), supported the research.

Author affiliations: [a]Department of Entomology, College of Agriculture, Food and Environment, University of Kentucky, Lexington, KY 40546

Author contributions: X.C., J.K., S.K.A., and S.R.P. designed research; X.C., J.K., and S.K.A. performed research; X.C., S.K.A., and S.R.P. analyzed data; and X.C., J.K., and S.R.P. wrote the paper.

1. L. M. Riddiford, Rhodnius, golden oil, and Met: A history of juvenile hormone research. *Front. Cell Dev. Biol.* **8**, 679 (2020).
2. X. Pan, R. P. Connacher, M. B. O'Connor, Control of the insect metamorphic transition by ecdysteroid production and secretion. *Curr. Opin. Insect Sci.* **43**, 11–20 (2021).
3. K. Hiruma, Y. Kaneko, Hormonal regulation of insect metamorphosis with special reference to juvenile hormone biosynthesis. *Curr. Topics Dev. Biol.* **103**, 73–100 (2013).
4. M. Jindra, S. R. Palli, L. M. Riddiford, The juvenile hormone signaling pathway in insect development. *Ann. Rev. Entomol.* **58**, 181–204 (2013).
5. T. Kayukawa, A. Jouraku, Y. Ito, T. Shinoda, Molecular mechanism underlying juvenile hormone-mediated repression of precocious larval-adult metamorphosis. *Proc. Natl. Acad. Sci. U.S.A.* **114**, 1057–1062 (2017).
6. T. Kayukawa *et al.*, Krüppel homolog 1 inhibits insect metamorphosis via direct transcriptional repression of Broad-complex, a pupal specifier gene. *J. Biol. Chem.* **291**, 1751–1762 (2016).
7. B. Konopova, M. Jindra, Juvenile hormone resistance gene Methoprene-tolerant controls entry into metamorphosis in the beetle Tribolium castaneum. *Proc. Natl. Acad. Sci. U.S.A.* **104**, 10488–10493 (2007).
8. B. Konopova, V. Smykal, M. Jindra, Common and distinct roles of juvenile hormone signaling genes in metamorphosis of holometabolous and hemimetabolous insects. *PloS one* **6**, e28728 (2011).
9. C. Minakuchi, T. Namiki, T. Shinoda, Krüppel homolog 1, an early juvenile hormone-response gene downstream of Methoprene-tolerant, mediates its anti-metamorphic action in the red flour beetle Tribolium castaneum. *Dev. Biol.* **325**, 341–350 (2009).
10. T. Daimon, M. Uchibori, H. Nakao, H. Sezutsu, T. Shinoda, Knockout silkworms reveal a dispensable role for juvenile hormones in holometabolous life cycle. *Proc. Natl. Acad. Sci. U.S.A.* **112**, E4226–E4235 (2015).
11. V. Smykal *et al.*, Importance of juvenile hormone signaling arises with competence of insect larvae to metamorphose. *Dev. Biol.* **390**, 221–230 (2014).
12. D. Martín, S. Chafino, X. Franch-Marro, How stage identity is established in insects: The role of the metamorphic gene network. *Curr. Opin. Insect Sci.* **43**, 29–38 (2021).
13. J. W. Truman, L. M. Riddiford, Chinmo is the larval member of the molecular trinity that directs Drosophila metamorphosis. *Proc. Natl. Acad. Sci. U.S.A.* **119**, e2201071119 (2022).
14. C. Dillard, K. Narbonne-Reveau, S. Foppolo, E. Lanet, C. Maurange, Two distinct mechanisms silence chinmo in Drosophila neuroblasts and neuroepithelial cells to limit their self-renewal. *Development* **145**, dev154534 (2018).
15. S. Zhu *et al.*, Gradients of the Drosophila Chinmo BTB-zinc finger protein govern neuronal temporal identity. *Cell* **127**, 409–422 (2006).
16. M. H. Syed, B. Mark, C. Q. Doe, Steroid hormone induction of temporal gene expression in Drosophila brain neuroblasts generates neuronal and glial diversity. *Elife* **6**, e26287 (2017).
17. K. Doggett *et al.*, BTB-zinc finger oncogenes are required for Ras and Notch-driven tumorigenesis in Drosophila. *PLoS One* **10**, e0132987 (2015).
18. K. Narbonne-Reveau, C. Maurange, Developmental regulation of regenerative potential in Drosophila by ecdysone through a bistable loop of ZBTB transcription factors. *PLoS Biol.* **17**, e3000149 (2019).

19. S. Chafino, P. Giannios, J. Casanova, D. Martín, X. Franch-Marro, Antagonistic role of the BTB-zinc finger transcription factors Chinmo and broad-complex in the juvenile/pupal transition and in growth control. *Elife* **12**, e84648 (2023).
20. L. M. Riddiford, M. Ashburner, Effects of juvenile hormone mimics on larval development and metamorphosis of Drosophila melanogaster. *Gen. Comp. Endocrinol.* **82**, 172–183 (1991).
21. X. Chen, S. R. Palli, Hyperactive piggyBac transposase-mediated germline transformation in the fall armyworm, Spodoptera frugiperda. *JoVE* **175**, e62714 (2021).
22. X. Chen, S. R. Palli, Development of multiple transgenic CRISPR/Cas9 methods for genome editing in the fall armyworm, *Spodoptera frugiperda*. *J. Pest Sci.* **96**, 1637–1650 (2023).
23. J. Chang *et al.*, Genome-wide CRISPR screening reveals genes essential for cell viability and resistance to abiotic and biotic stresses in Bombyx mori. *Genome Res.* **30**, 757–767 (2020).
24. T. Kayukawa *et al.*, Hormonal regulation and developmental role of Krüppel homolog 1, a repressor of metamorphosis, in the silkworm Bombyx mori. *Dev. Biol.* **388**, 48–56 (2014).
25. E. Ureña, S. Chafino, C. Manjón, X. Franch-Marro, D. Martín, The occurrence of the holometabolous pupal stage requires the interaction between E93, Krüppel-Homolog 1 and Broad-Complex. *PLoS Genet.* **12**, e1006020 (2016).
26. H. Mabashi-Asazuma, D. L. Jarvis, CRISPR-Cas9 vectors for genome editing and host engineering in the baculovirus–insect cell system. *Proc. Natl. Acad. Sci. U.S.A.* **114**, 9068–9073 (2017).
27. L. Safranek, L. M. Riddiford, The biology of the black larval mutant of the tobacco hornworm, Manduca sexta. *J. Insect Physiol.* **21**, 1931–1938 (1975).
28. G. H. Zhu, Y. Jiao, S. Chereddy, M. Y. Noh, S. R. Palli, Knockout of juvenile hormone receptor, Methoprene-tolerant, induces black larval phenotype in the yellow fever mosquito, Aedes aegypti. *Proc. Natl. Acad. Sci. U.S.A.* **116**, 21501–21507 (2019).
29. H. Bai, P. Ramaseshadri, S. R. Palli, Identification and characterization of juvenile hormone esterase gene from the yellow fever mosquito, Aedes aegypti. *Insect Biochem. Mol. Biol.* **37**, 829–837 (2007).
30. A. Tan, H. Tanaka, T. Tamura, T. Shiotsuki, Precocious metamorphosis in transgenic silkworms overexpressing juvenile hormone esterase. *Proc. Natl. Acad. Sci. U.S.A.* **102**, 11751–11756 (2005).
31. Z. Zhang *et al.*, Depletion of juvenile hormone esterase extends larval growth in Bombyx mori. *Insect Biochem. Mol. Biol.* **81**, 72–79 (2017).
32. I. González-Santoyo, A. Córdoba-Aguilar, Phenoloxidase: A key component of the insect immune system. *Entomol. Exp. Appl.* **142**, 1–16 (2012).
33. K. Hiruma, L. M. Riddiford, The molecular mechanisms of cuticular melanization: The ecdysone cascade leading to dopa decarboxylase expression in Manduca sexta. *Insect Biochem. Mol. Biol.* **39**, 245–253 (2009).
34. T. Shinoda, K. Itoyama, Juvenile hormone acid methyltransferase: A key regulatory enzyme for insect metamorphosis. *Proc. Natl. Acad. Sci. U.S.A.* **100**, 11986–11991 (2003).
35. F. G. Noriega, Juvenile hormone biosynthesis in insects: What is new, What do we know, and What questions remain? *Int. Sch. Res. Notices* **2014**, 967361 (2014).
36. M. Hejnikova, M. Paroulek, M. Hodkova, Decrease in Methoprene tolerant and Taiman expression reduces juvenile hormone effects and enhances the levels of juvenile hormone circulating in males of the linden bug Pyrrhocoris apterus. *J. Insect Physiol.* **93**, 72–80 (2016).
37. M. Gijbels, C. Lenaerts, J. Vanden Broeck, E. Marchal, Juvenile Hormone receptor Met is essential for ovarian maturation in the Desert Locust, Schistocerca gregaria. *Sci. Rep.* **9**, 10797 (2019).
38. J. Leyria, I. Orchard, A. B. Lange, Impact of JH signaling on reproductive physiology of the classical insect model, Rhodnius prolixus. *Int. J. Mol. Sci.* **23**, 13832 (2022).
39. Y. Obara *et al.*, Pupal commitment and its hormonal control in wing imaginal discs. *J. Insect Physiol.* **48**, 933–944 (2002).
40. G. Jones, N. Brown, M. Manczak, S. Hiremath, F. C. Kafatos, Molecular cloning, regulation, and complete sequence of a hemocyanin-related, juvenile hormone-suppressible protein from insect hemolymph. *J. Biol. Chem.* **265**, 8596–8602 (1990).
41. G. Jones, M. Wozniak, D. Jones, Newly identified, basic hemolymph proteins from noctuid species. *Biochem. Biophys. Res. Commun.* **146**, 265–269 (1987).
42. V. Exner, P. Taranto, N. Schönrock, W. Gruissem, L. Hennig, Chromatin assembly factor CAF-1 is required for cellular differentiation during plant development. *Development (Cambridge, England)* **133**, 4163–4172 (2006).
43. M. Clémot, A. Molla-Herman, J. Mathieu, J. R. Huynh, N. Dostatni, The replicative histone chaperone CAF1 is essential for the maintenance of identity and genome integrity in adult stem cells. *Development (Cambridge, England)* **145**, dev161190 (2018).
44. A. Auger *et al.*, Eaf1 is the platform for NuA4 molecular assembly that evolutionarily links chromatin acetylation to ATP-dependent exchange of histone H2A variants. *Mol. Cell Biol.* **28**, 2257–2270 (2008).
45. R. Parthasarathy, S. R. Palli, Stage-specific action of juvenile hormone analogs. *J. Pestic. Sci.* **46**, 16–22 (2021).
46. M. Kamimura, M. Kiuchi, Applying fenoxycarb at the penultimate instar triggers an additional ecdysteroid surge and induces perfect extra larval molting in the silkworm. *Gen. Comp. Endocrinol.* **128**, 231–237 (2002).
47. H. Khong, K. B. Hattley, Y. Suzuki, The BTB transcription factor, Abrupt, acts cooperatively with Chronologically inappropriate morphogenesis (Chinmo) to repress metamorphosis and promotes leg regeneration. *Dev. Biol.* **509**, 70–84 (2024).
48. Q. He, Y. Zhang, Kr-h1, a cornerstone gene in insect life history. *Front. Physiol.* **13**, 905441 (2022).
49. M. J. Niederhuber, D. J. McKay, Mechanisms underlying the control of dynamic regulatory element activity and chromatin accessibility during metamorphosis. *Curr. Opin. Insect Sci.* **43**, 21–28 (2021).
50. C. M. Uyehara *et al.*, Hormone-dependent control of developmental timing through regulation of chromatin accessibility. *Genes Dev.* **31**, 862–875 (2017).
51. S. L. Nystrom, M. J. Niederhuber, D. J. McKay, Expression of E93 provides an instructive cue to control dynamic enhancer activity and chromatin accessibility during development. *Development (Cambridge, England)* **147**, dev181909 (2020).
52. X. Chen, S. R. Palli, Midgut-specific expression of CYP321A8 P450 gene increases deltamethrin tolerance in the fall armyworm Spodoptera frugiperda. *J. Pest Sci.* **96**, 1611–1623 (2023).
53. X. Chen, S. Chereddy, D. Gurusamy, S. R. Palli, Identification and characterization of highly active promoters from the fall armyworm, Spodoptera frugiperda. *Insect Biochem. Mol. Biol.* **126**, 103455 (2020).
54. A. Roy, S. R. Palli, Epigenetic modifications acetylation and deacetylation play important roles in juvenile hormone action. *BMC Genomics* **19**, 934 (2018).
55. X. Chen, J. Koo, S. K. Arya, S. R. Palli, Data from "Chronologically inappropriate morphogenesis (Chinmo) is required for maintenance of larval stages of fall armyworm." NCBI. https://dataview.ncbi.nlm.nih.gov/object/PRJNA1168504. Deposited 3 October 2024.
56. K. Belhocine, L. DeMare, O. Habern, Single-cell multiomics: Simultaneous epigenetic and transcriptional profiling: 10x genomics shares experimental planning and sample preparation tips for the chromium single cell multiome ATAC+ gene expression system *Genet. Eng. Biotechn. N.* **41**, 66–68 (2021).
57. X. Chen, J. Koo, S. K. Arya, S. R. Palli, Data from "Chronologically inappropriate morphogenesis (Chinmo) is required for maintenance of larval stages of fall armyworm." NCBI. https://dataview.ncbi.nlm.nih.gov/object/PRJNA1168511. Deposited 3 October 2024.
58. T. Stuart, A. Srivastava, S. Madad, C. A. Lareau, R. Satija, Single-cell chromatin state analysis with Signac. *Nat. Methods* **18**, 1333–1341 (2021).
59. J. M. Gaspar, Improved peak-calling with MACS2. bioXriv [Preprint] (2018). https://doi.org/10.1101/496521 (Accessed 17 December 2018).
60. A. Khan *et al.*, JASPAR 2018: Update of the open-access database of transcription factor binding profiles and its web framework. *Nucleic Acids Res.* **46**, D1284 (2018).
61. W. Huber *et al.*, Orchestrating high-throughput genomic analysis with Bioconductor. *Nat. Methods* **12**, 115–121 (2015).
62. R. C. Gentleman *et al.*, Bioconductor: Open software development for computational biology and bioinformatics. *Genome Biol.* **5**, R80 (2004).
63. T. L. Bailey *et al.*, MEME SUITE: Tools for motif discovery and searching. *Nucleic Acids Res.* **37**, W202–208 (2009).